J. Membrane Biol. 187, 117–133 (2002)
DOI: 10.1007/s00232-001-0156-4

The Journal of
Membrane
Biology

Influence of Amino-Terminal Structures on Kinetic Transitions between Several Closed and Open States in Human *erg* K^+ Channels

D. Gómez-Varela, P. de la Peña, J. García*, T. Giráldez, F. Barros
Departamento de Bioquímica y Biología Molecular, Facultad de Medicina, Universidad de Oviedo, Edificio Santiago Gascón, Campus del Cristo, E-33006, Oviedo, Spain
*Departamento de Física, Facultad de Ciencias, Universidad de Oviedo, C/ Calvo Sotelo s/n, E-33007, Oviedo, Spain

Received: 14 November 2001/Revised: 1 February 2002

Abstract. Gating kinetics of human *ether-a-go-go* (*eag*)-*related* gene (HERG) K^+ channel expressed in *Xenopus* oocytes was studied using non-inactivating channel variants carrying different structural modifications in the amino terminus. A kinetics model was elaborated to describe the behavior of full-length channels, that includes at least three open states besides the three closed states previously proposed. Deletion of the HERG-specific proximal domain (HERG Δ138–373) accelerated all individual forward transitions between closed states. Whereas relatively large amplitude depolarizations were required to drive full-length HERG channels to more distal open states, these were reached more easily in channels without proximal domain. Alteration of the initial *eag*/PAS domain by introduction of a short amino-acid sequence at the beginning of the amino terminus did not alter transitions between closed states, but prevented the channels from reaching the farthest open states that determine slower deactivation rates. This indicates that the presence of specific amino-terminal structures can be correlated with the occurrence of distinctive molecular transitions. It also demonstrates that both proximal and *eag*/PAS domains in the amino terminus contribute to set the gating characteristics of HERG channels.

Key words: HERG — Potassium channel — Kinetic model — Human heart — *Xenopus* oocytes

Correspondence to: F. Barros; email: fbarros@correo.uniovi.es

Introduction

Human *ether-a-go-go*-related gene (HERG) and HERG-like potassium channels play a key role setting the electrical behavior of a variety of cell types (Barros et al., 1994, 1997; Arcangeli et al., 1997; Zhou et al., 1998; Akbarali et al., 1999; Bauer et al., 1999; Schäfer et al., 1999; Cherubini et al., 2000; Emmi et al., 2000; Overholt et al., 2000; Rosati et al., 2000). The best documented implication of HERG relates to cardiac ventricular cells, in which this channel mediates the repolarizing current I_{Kr}. This current participates in the repolarization phase of the cardiac action potential, and subsequently in control of the spike and interspike intervals (Smith, Baukrowitz & Yellen, 1996; Zhou et al., 1998). Hence mutations in the h-*erg* gene have been recognized as the cause of certain forms of familial long-QT syndrome (Curran et al., 1995; Sanguinetti et al., 1995; Spector et al., 1996*a*), and pharmacological blockade of HERG is also the determinant of acquired forms of this syndrome (Roden et al., 1996; Spector et al., 1996*a*).

Crucial kinetic determinants of HERG physiological roles are the existence of a particularly slow activation rate that overlaps with a rapid and voltage-dependent inactivation process, limiting the level of outward current upon depolarization, and a particularly slow deactivation rate following the fast recovery of inactivation upon repolarization (Sanguinetti et al., 1995; Trudeau et al., 1995; Schönherr & Heinemann, 1996; Smith et al., 1996; Spector et al., 1996*b*; Wang et al., 1997). This makes HERG functionally appear as an inward rectifier, although its molecular structure of six membrane-spanning domains and an S4 charged region corresponds to that of a typical depolarization-activated channel (Warmke & Ganetzky, 1994).

The amino-acid sequence of HERG shows that it has the longest amino terminus of any potassium channel, mainly due to the presence of a long stretch of residues extending from about position 135 to about position 366 (the "proximal" domain; *see* Viloria et al., 2000) that follows an initial domain (the *eag* or PAS domain) conserved in the *eag* family. Although the best described functional role of K^+ channel N-terminal domain(s) is to provide the ball for N-type inactivation (Hoshi et al., 1990), recent work has implicated the N-terminus of different channels in regulation not only of channel assembly, but also of voltage dependence and/or activation kinetics (Schönherr & Heinemann, 1996; Spector et al., 1996*b*; Marten & Hoshi, 1997; Pascual et al., 1997; Terlau et al., 1997; Cushman et al., 2000; Minor et al., 2000). Previous work from several laboratories indicated that the interaction of the *eag*/PAS domain with the channel core acts as a molecular brake that determines the slow HERG deactivation kinetics (Cabral et al., 1998; Wang et al., 1998; Sanguinetti & Xu, 1999). However, the molecular determinant(s) of HERG activation slowness are still poorly defined. The crystal structure of the *eag*/PAS domain has been resolved (Cabral et al., 1998). Interestingly, the initial 25 residues most conserved in this domain that remain disordered in the crystal seem to constitute a key factor to specifically stabilize the open state and thus slow HERG closing (Wang, Myers & Robertson, 2000). Nevertheless, the exact nature of the interactions between this domain and either the channel core or the remaining amino-terminal sequences is not known. In a recent work, we showed that the presence of the proximal domain exclusive of HERG constitutes an essential determinant of its slow activation gating (Viloria et al., 2000). Our results suggested that the need to adequately modify the conformation of the proximal domain acts as a constraining factor on efficient progress through the activation pathway, limiting or slowing down the interaction of the *eag* domain with the channel.

In this report, the activation and deactivation gating characteristics of HERG are deeply explored using non-inactivating S620T channel variants carrying different structural modifications in the amino terminus. This led us to elaborate a kinetics model to describe the behavior of full-length channels, which includes at least three open states along with the three closed states previously proposed (Wang et al., 1997; Kiehn, Lacerda & Brown, 1999). Such a model reproduced not only the sigmoid time course of HERG activation, but also the complex time course of deactivation, including the dependence of closing rates on the magnitude and/or duration of previous depolarization (Viloria et al., 2000). Performance of similar kinetic analysis with channels without proximal domain indicates that all individual transitions between closed states are accelerated by such a domain removal and that proximal domain-deleted channels move more easily through the activation pathway up to the more distal open states. However, whereas a variant carrying an alteration in the *eag*/PAS domain shows transitions between closed states similar to those of wild-type channels, it seems unable to reach the farthest open states that determine slower deactivation rates. This allows us to associate the presence of specific amino-terminal structures with the occurrence of distinctive molecular transitions. It also emphasizes the relevance of both proximal and *eag*/PAS domains of the amino terminus setting HERG gating characteristics, and hence its physiological role in cardiac, neuronal and neuroendocrine cells.

Materials and Methods

Generation of Channel Mutants

Unless indicated, all experiments were performed on HERG channels made incapable of inactivation by substitution of serine with threonine in position 620 (S620T; Ficker et al., 1998; Viloria et al., 2000). We always use "wild-type" in the graphs and throughout the text to refer to full-length S620T channels, and "Δ138–373" or "H3HA" for S620T channels carrying additional modifications in the amino terminus. The procedure for generation of the Δ138–373 channel lacking the proximal domain has been detailed elsewhere (Viloria et al., 2000). To construct the H3HA variant, a nine-amino-acid hemagglutinin (HA) epitope tag recognized by the monoclonal antibody 12CA5 was placed at the beginning of the amino terminus by inserting in the *Hind*III site of the HERG clone a double-stranded oligonucleotide (5′-AG CTT AGG ATG TAC CCT TAC GAC GTT CCT GAC TAC GCT A-3′) that contains the recognition site for *Hind*III and an ATG followed by the HA epitope sequence.

Plasmids and Preparation of CRNA

The plasmid containing the cDNA for the HERG channel was a generous gift of Dr. E. Wanke (University of Milano, Milano, Italy). Plasmids were linearized and capped cRNA was in vitro synthesized from the linear cDNA templates by standard methods using SP6 RNA polymerase as described (de la Peña et al., 1992).

Oocyte Expression and Solutions

Procedures for frog anaesthesia and surgery, oocyte obtaining and microinjection have been detailed elsewhere (Barros et al., 1998). Oocytes were maintained in OR-2 medium (in mM: NaCl 82.5, KCl 2, $CaCl_2$ 2, $MgCl_2$ 2, Na_2HPO_4 1, HEPES 10, at pH 7.5). Cytoplasmic microinjections were performed with 30–50 nl of in vitro synthesized cRNA per oocyte. HERG currents were studied in manually defolliculated oocytes (de la Peña et al., 1992; Barros et al., 1998). Recordings were obtained in standard OR-2 or in high-K^+ medium in which 50 mM KCl substituted an equivalent amount of NaCl. Functional expression was typically assessed 2–3 days after microinjection.

Data Acquisition and Analysis

Recordings were made at room temperature using the two-electrode voltage-clamp method with a Turbo TEC 01C (NPI, Tamm, Germany) amplifier as described previously (Barros et al., 1998; Viloria et al., 2000). Membrane potential was typically clamped at −80 mV, and at −100 or −110 mV for Δ138–373 channels to compensate for the left-shift in voltage dependence of activation caused by the deletion (Viloria et al., 2000). Stimulation and data acquisition were controlled with Pulse + PulseFit software (HEKA Elektronic, Lambrecht, Germany) running on Macintosh computers. Ionic currents sampled at 1 kHz were elicited using the voltage protocols indicated in the graphs. Exponential fits to ionic currents were performed with the programs PulseFit (HEKA Elektronic) and Igor-Pro (WaveMetrics, LakeOswego, OR). For fitting to a given kinetic scheme, previously reported rate constants (Wang et al., 1998) were initially used. Rate constants for additional non-defined transitions were first roughly set by trial and error. Then, the rates were iteratively refined with a Marquardt optimization procedure using Model Maker (Cherwell Scientific, Oxford, U.K.) or a custom-made routine written on Mathematica (Wolfram Research, Champaign, IL). Model parameters were confirmed using a simulated annealing algorithm to find global minimums (Irvine, Jafri & Winslow, 1999). Numerical accuracy was confirmed by demonstrating insensitivity to step size. Goodness of fits was evaluated by inspecting the residuals and comparing χ^2 values statistically. In all cases, fits started as soon as the clamp settled. Current modeling was performed assuming linear Markov models as shown below. Voltage-dependent forward and backward rates were assumed to be of the form:

$$\alpha_{ij} = A_{ij} \exp(B_{ij} \cdot Em) \text{ and } \beta_{ij} = A_{ij} \exp(-B_{ij} \cdot Em), \quad (1)$$

respectively, where A_{ij} is the rate at 0 mV and Em is the membrane potential in millivolts. Current simulations were performed by solving the Q matrix (Colquhoun & Hawkes, 1995) with the program Mathematica running in a Macintosh computer. Data from simulations and experimentally obtained current records were superimposed and shown on the graphs using Igor-Pro. Data are presented as means ± SE for the number of oocytes indicated in the graphs.

Results

Deletion of HERG Proximal Domain Accelerates Transitions Between Closed States of the Channel

In a previous study, we found that the proximal domain (*see* above) of HERG plays a key role controlling current activation (Viloria et al., 2000). Our data suggested that removal of this domain accelerates transitions through closed states. To determine what specific transitions could be influenced by the presence of the proximal domain, we initially quantified and compared the voltage dependence of the activation parameters in channels with and without this domain by fitting the upper half of the current records to an exponential and a delay (Figs. 1, 2). To prevent any influence of inactivation and/or inactivation recovery steps in the results, all the experiments were conducted with S620T channels from which inactivation has been completely removed by substitution of serine with threonine in position 620 (Ficker et al., 1998).

Assuming a sequential gating scheme as previously proposed for HERG (Wang et al., 1997; Kiehn et al., 1999)

$$C_1 \underset{\beta_{21}}{\overset{\alpha_{12}}{\leftrightarrows}} C_2 \underset{k_b}{\overset{k_f}{\leftrightarrows}} C_3 \underset{\beta_{43}}{\overset{\alpha_{34}}{\leftrightarrows}} O_4$$

the time constant of the exponential fit at positive voltages is a measure of the reciprocal value of the slowest rate constant in the activation pathway, and the delay is the reciprocal value of the sum of all the rest of the rate constants (Schoppa & Sigworth, 1998; Gonzalez et al., 2000). As shown in Fig. 1, channels lacking the proximal domain showed smaller delays at a given voltage than wild-type channels. The leftward shift in the delay caused by proximal domain removal is not due solely to the shift in voltage dependence of activation induced by the deletion, since, whereas only a ≈20 mV shift to the left is observed in the steady-state activation voltage dependence of Δ138–373 channels (Viloria et al., 2000), the voltage dependence of the delay is displaced ≈50 mV to negative values (Fig. 1*B*). Thus clearly one or more of the forward rate constants are affected by removal of the proximal domain.

A unique feature of the HERG activation process among other voltage-gated K^+ channels is the presence of a voltage-insensitive step preceding the final voltage-dependent transition that communicates with the open state(s) (Liu et al., 1996; Wang et al., 1997). This makes the plots of the rates during the late phase of activation appear as a saturating function of voltage at positive potentials at which such a voltage-insensitive step becomes dominant (Wang et al., 1997). Thus we performed a quantitative comparison of the effects of proximal domain deletion on this saturating forward time constant using the values of the time constants of activation obtained from the fits to the upper half of the rising phase of the current records. As shown in Fig. 2, the time constants obtained from mono-exponential fits to the late phase of activation became voltage-insensitive at positive potentials, reaching an asymptotic value of 62 msec in full-length S620T channels. A similar value of 68 msec has been reported previously using normally inactivating channels (Wang et al., 1997).

When a similar analysis was performed with channels lacking the proximal domain, the voltage-independent transition was clearly accelerated, as evidenced by the reduction of the saturating time constant to 17 msec. Interestingly, although the single-exponential fits to the data quite accurately followed the current time course in wild-type channels for 300–400-msec short depolarizations up to +60 mV, clear deviations between the currents and

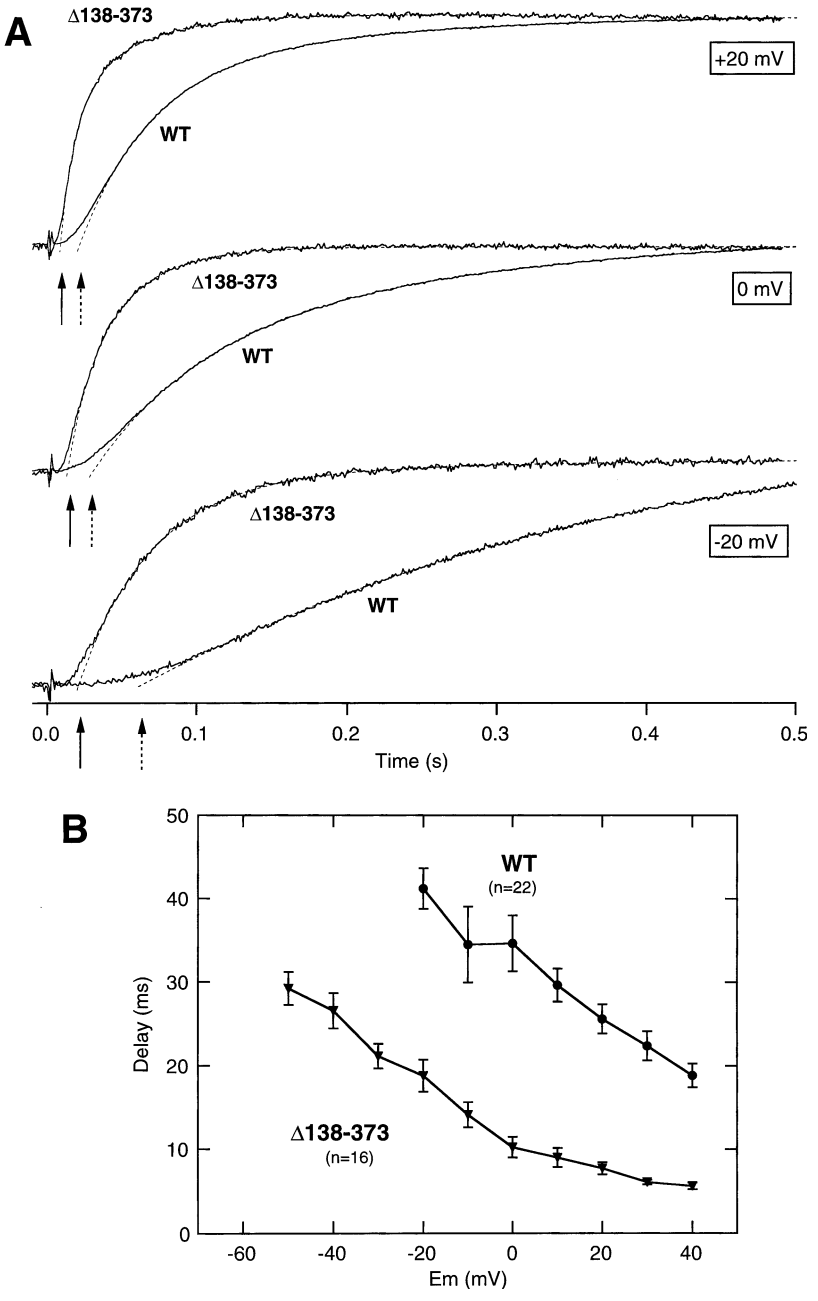

Fig. 1. Effect of proximal domain deletion on current delay of the sigmoidal time course of HERG activation. (*A*) The upper half of the macroscopic HERG current elicited by depolarization to −20, 0 and +20 mV as indicated, was fitted to a single exponential (*dotted lines*). The extrapolation of the fit to zero current (*arrows*) was used to estimate the delay in activation that corresponds to the reciprocal value of the sum of all the rate constants other than that determining the slowest step of the process (Schoppa and Sigworth, 1998; Gonzalez et al., 2000). Current magnitudes have been normalized to their maximal amplitude during the depolarization pulse. Note that although only the initial 0.5 sec of the traces are shown for a better visual comparison of differences in delay, depolarizations of 3 sec were used with wild-type channels to reach steady-state at negative voltages (e.g., −20 mV) and to perform the fits. (*B*) Voltage dependence of the delay taken from current measurements as in panel *A*. Data are shown for wild-type (*circles*) and proximal domain-deleted (Δ138–373, *triangles*) channels. In all cases, non-inactivating S620T channels were used (*see* Methods). Analysis range was limited up to +40 mV to prevent the influence of Na^+ ion block at very positive potentials (Ficker et al., 1998). Note that the apparent saturation of delay values at positive voltages in Δ138–373 channels could be due, at least in part, to temporal limitations of the voltage clamp setting membrane voltage. Almost identical results were obtained after performing a bi-exponential fit to the current data.

the fits were observed in Δ138–373 channels above 0 mV even with these short depolarizations. These deviations became also apparent when mono-exponential fits were attempted with wild-type records in response to longer depolarizing pulses. In both cases, accuracy of the fit was strongly improved by using a bi-exponential that included a slow second component (Fig. 2*A*, right panels). The possible significance of such a slower component that otherwise accounted for near 10% of the whole amplitude, will be discussed below. Nevertheless, when the variation of the time constant corresponding to the major fast component was studied at different voltages, only a relatively small variation from 62 to 41 msec was obtained for full-length channels. However, the saturation of the time constant in proximal domain-deleted channels reached a value of 6 msec, again clearly smaller than that observed from full-length channels. Finally, asymptotic values of 32 and 19 msec were obtained for wild-type and Δ138–373 channels, when oocytes were bathed in high-K^+ medium to minimize current rectification at positive voltages and to extend the range of analysis up to +80 mV (inset of Fig. 2*B*). Altogether, this indicates that removal of the proximal domain accelerates between two- and seven-fold the voltage-insensitive transition between C_2 and C_3 in the HERG activation pathway.

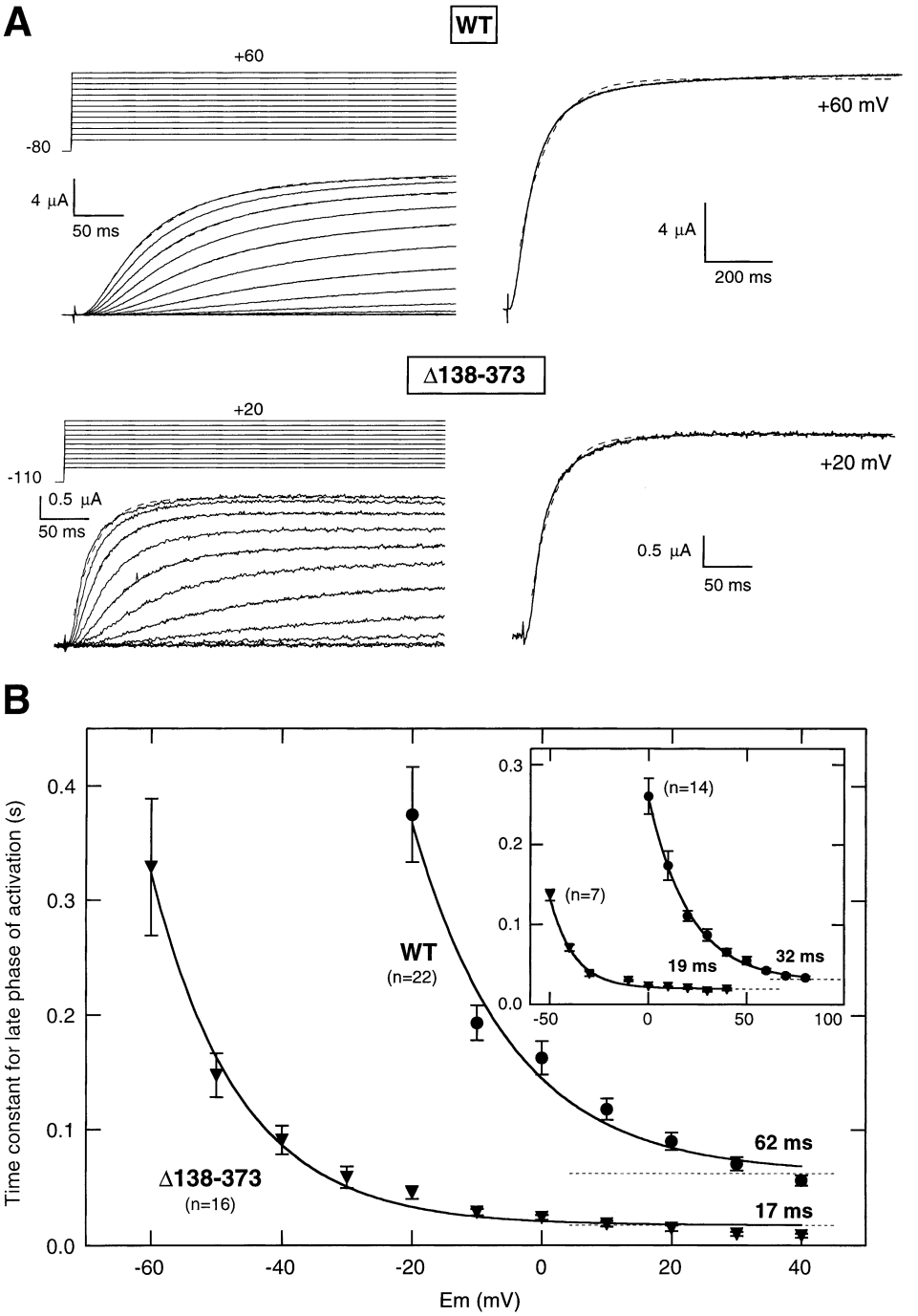

Fig. 2. Effect of proximal domain removal on apparent saturation in the late phase of activation at positive potentials. (*A*) Ionic currents shown at the top were recorded following depolarizing pulses to the indicated potentials applied to S620T full-length channels (WT) or channels lacking the proximal domain (Δ138–373). The late phase of the current records was fitted with a single exponential (*dashed lines*) starting near the time at which current had reached ~40–50% of the maximum. Only fits to currents obtained every two pulses starting at the more positive voltage are shown for simplicity. Note the quality of the mono-exponential fits to WT current records up to +60 mV when current time course was limited to the initial 400 msec (*left*), but not to currents lasting for 1 second or longer (*right*). Note also the poor accuracy of the single-exponential fit to Δ138–373 macroscopic currents at +20 mV even when the analysis was limited to only 400 msec. In both cases, indistinguishable fit and current time courses were obtained when a double-exponential was used (also shown superimposed to the wild-type and Δ138–373 current records on the right). (*B*) The time constants from *A* are plotted as a function of test potential. Values of the time constants obtained from single-exponential fits to currents obtained following short depolarizing pulses are shown in the main panel. Plots of time constants after a similar analysis from oocytes bathed in high-K^+ medium to minimize current rectification at positive voltages and to extend the range of analysis up to +80 mV are shown in the inset. In all cases the time constants of activation showed a near exponential dependence on membrane potential as shown by the curve fitted to the data. This exponential [$y = A + B \exp(C \cdot x)$] did not decay to zero at positive potentials, but reached an asymptotic value (*dotted lines*) as indicated.

Effect of Proximal Domain Removal on Individual Voltage-Dependent Transitions Along the Activation Pathway

Comparison of time constants for the voltage-independent C_2 to C_3 transition (Fig. *2*) and delay values as those of Fig. 1 (corresponding to rate constants faster than the rate-limiting one) indicates that, at least for wild-type channels, the voltage-independent step constitutes the slowest transition at depolarized voltages above −20 mV. To obtain the individual values of the rest of time constants and to know the possible effects on them of proximal domain removal, we fitted the current-activation time course to the aforementioned three-closed-states model (Fig. 3). Averaged currents from fourteen oocytes were used for the analysis. As for normally inactivating wild-type channels (Wang et al., 1997), a two-closed-states model was not adequate to describe the data and models with more than three closed states did not improve substantially the quality of the fits (*not shown*). Once optimized as stated in Methods, the best fit to current records at different voltages (Fig. 3*A*) was used to obtain the exponential expressions (equation 1, *see* Methods) that better matched the variation of voltage-dependent forward and backward rate constants as a function of voltage (Fig. 3*B*, left panel). This yielded the numerical values shown in the left panel of Fig. 3*C* for the different individual transitions. Very similar parameters were also obtained when the analysis was repeated in every individual cell and the averaged data values were used to obtain the numerical values of the exponential expressions (right panels in Fig. 3*C*, *D*). Interestingly, even although all forward and backward time constants are freely varied during optimization of current fitting, the variation with voltage of k_f and k_b as predicted by the model was very small. This adds further support to the existence of a particularly voltage-insensitive step during the activation sequence of HERG. Using this procedure, a value of 36–38 msec was obtained for the saturating voltage-independent time constant ($1/k_f$), which reasonably agreed with the time constant experimentally determined from saturation of the exponential fits to the late phase of activation (30–60 msec, *see* Fig. 2). In fact, very similar exponential expressions were obtained when the dynamic characteristics of the model were constrained fixing the k_f rate to the values experimentally obtained (*not shown*). Finally, the voltage-dependent transition connecting backward the open and the last closed state (β_{43}) becomes particularly slow at positive potentials. This precluded an accurate estimation of such a constant from fits at the positive voltages used to study current activation. Therefore, values obtained from fits to activating currents can be regarded as only approximates. For this reason the magnitude of this constant and its voltage dependence were obtained from the time course of deactivating tails at more negative voltages (*see below*).

The results obtained by application of the three-closed-states model to current records of proximal domain-deleted Δ138–373 channels are shown in Fig. 4. Again, a two-closed-states model was not adequate to describe the data and models with more than three closed states did not improve substantially the quality of the fits (*not shown*). Furthermore, as evidenced by the increased slope of the lines, the voltage-dependence of the forward voltage-dependent transitions in Δ138–373 channels was slightly larger than that of the wild-type ones. Finally, for a given voltage all three forward activation rates were clearly accelerated following removal of the proximal domain.

Existence of Multiple Open States as Evidenced by Deactivation Time-Course Dependence on the Amplitude of Previous Depolarization

As indicated above, use of long depolarization pulses indicated the existence of a small component of slow activation. This opens the possibility that additional closed states exist that could delay the opening of a small percentage of channels. However, we did not observe significant improvements in the fits to activation time courses when higher-order models containing more than three closed states were used (*not shown*). Alternatively, as previously shown for Kv1.5 channels, it could be also possible that the slow component is due to equilibration between multiple open states (Rich & Snyders, 1998). It is well known that HERG current deactivation follows a bi-exponential time course at negative voltages (Sanguinetti et al.,1995; Wang et al., 1998; Zhou et al., 1998; Sanguinetti & Xu, 1999; Viloria et al., 2000). Although compatible with a gating model involving multiple closed states (Correa & Bezanilla, 1994; Zagotta et al., 1994), this behavior could be associated also with the presence of several open states. Unfortunately, the presence of additional open states would not be detected by applying our fitting procedure exclusively to activation time courses if these open states show the same conductance. However, one prediction of a multiple-open-states system is that the deactivation time course would depend on the magnitude and/or duration of the activating pulses (Rich & Snyders, 1998). Since our previous data indicated that this is indeed the case (Viloria et al., 2000), we studied the fitting of the deactivation time course to different models containing one to four open states, following activation pulses to different potentials. As shown in Fig. 5, the model with only one open state fits very poorly the wild-type tail currents obtained after a depolarizing pulse of 400 msec at −30 mV. Substantial improvement in the fit

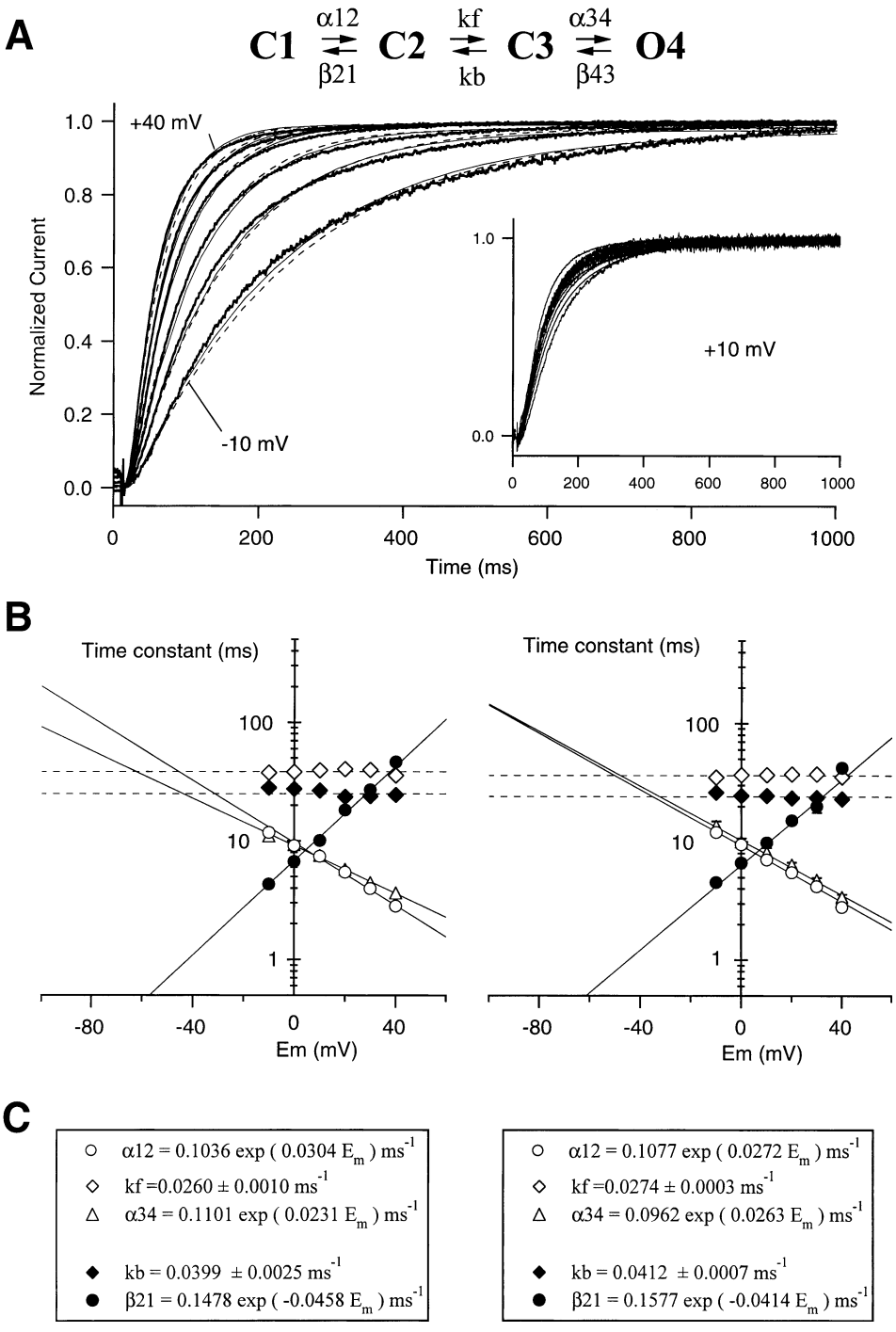

Fig. 3. Fitting of the sequential three-closed-states model to wild-type HERG activation. (*A*) The linear three-closed-states model shown at the top was used where *C*1, *C*2 and *C*3 are the three closed states in the activation pathway, *O*4 is the open and conducting state, α and β stand for the voltage-dependent forward and backward rate constants, respectively, and k_f/k_b represent the voltage-insensitive forward and backward rate constants. Fits (*thin continuous lines*) to time course of ionic currents (thick lines) recorded following depolarization steps between −10 and +40 mV are shown. Theoretical currents at every voltage as predicted by the model using the numerical expressions from panel *C* are also shown superimposed to the currents (*dashed lines*). Averaged currents from fourteen oocytes were normalized to maximum and used for fitting. An example of the normalized currents (at +10 mV) used for averaging is shown in the inset. In all cases, the small deviations in the time course of the fitted and the theoretical currents as compared with the averaged current remained well inside the area limited by the up and down SE values around every average data point. (*B*) Voltage dependence of the different rate constants as deduced from the fits using the three-closed-states model. The lines are fits to the data using an equation of the form $\alpha/\beta = A \exp(B \cdot Em)$ (*see* Methods), corresponding to the numerical values shown in panel *C*. *Open circles:* α_{12} *open triangles:* α_{34}; *closed circles:* β_{21}. Values of the backward β_{43} constant are not plotted due to inaccuracy of the estimations for this step using fits to activating currents at positive voltages (*see* text). Values for the voltage-independent time constants *kf* (*open diamonds*) and *kb* (*closed diamonds*) obtained at every voltage from the three-closed-states model fit, are also shown. The mean value of these constants at all voltages is indicated by dashed lines. (*C*) Numerical expressions used to define the different forward and backward rate constants as a function of membrane potential (*Em*) in millivolts. Data in the left panels of *C* and *D* correspond to the analysis performed with the averaged currents as in *A*. Data obtained with non-averaged currents from individual oocytes including the averaged time constants plus their respective errors are plotted in the right panels. In most cases the error bars are smaller than the symbols.

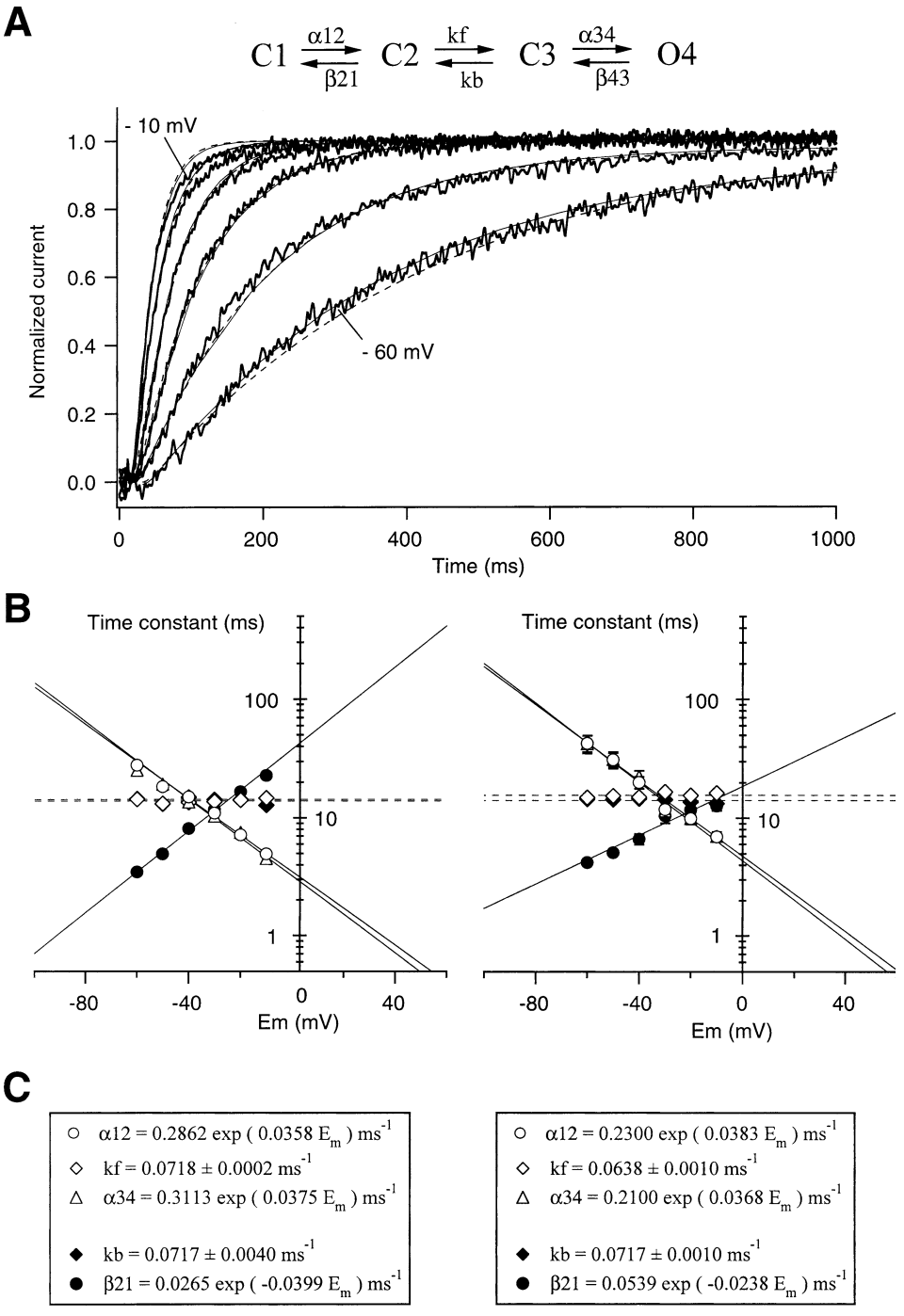

Fig. 4. Fitting of the sequential three-closed-states model to activation of HERG Δ138–373. The same nomenclature and fitting procedures as those indicated in the legend of Fig. 3 are used. In this case, the voltage range covered by depolarization steps goes from −60 to −10 mV, as indicated. The averaged value of the voltage-independent rate constants is signaled by horizontal dashed lines.

was obtained when a two-open-states model was used. Higher-order models failed to show any additional improvement, as evidenced by the similar value of residual errors. Interestingly, when a similar analysis was performed with tail currents following pulses to more depolarized voltages at which complete activation is achieved (e.g., +40 mV, Fig. 5*C*), poor fits were obtained again with a single-open-state model. Furthermore, although the use of the two-open-states model improved the visual quality of the fit, a three-open-states model better described the data, halving the total residual error. This indicates that increasing either the amplitude of depolarization or the depolarization time (*not shown*, *see* also Viloria

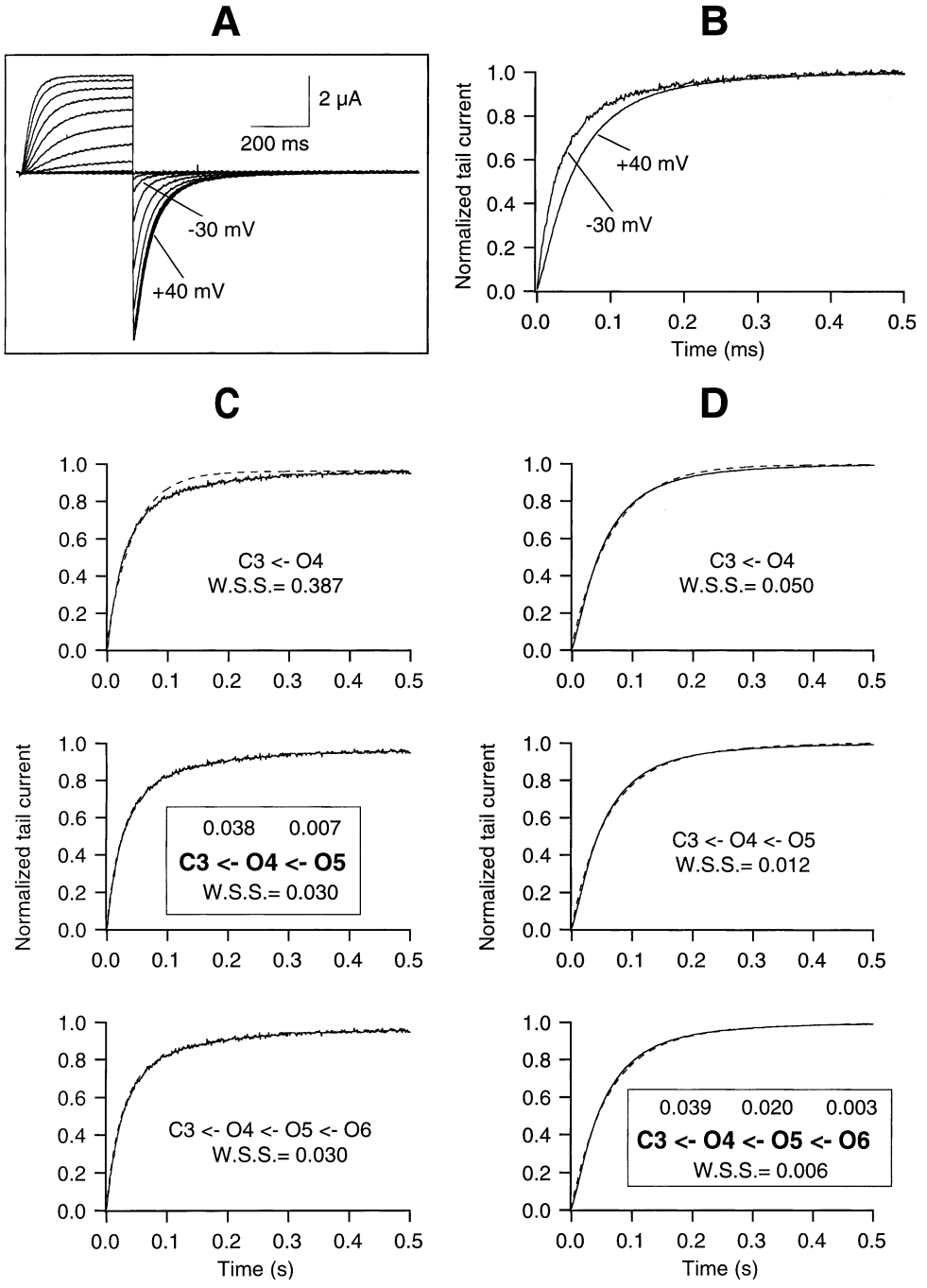

Fig. 5. Fitting of models with different number of open states to wild-type HERG deactivating tail currents as a function of previous depolarization voltage. (*A*) Family of currents in response to 0.4-msec depolarizations between −60 and +40 mV followed by 1-sec repolarizations to −100 mV. High-K^+ extracellular medium with 50 mM KCl was used to maximize tail current magnitude at negative repolarizing voltages. (*B*) Comparison of time course of tail currents recorded in response to depolarizing pulses to −30 and +40 mV. Normalized tail currents are shown corresponding to traces plotted in panel *A*. (*C*) Fits to time course of the tail current recorded at −110 mV following the 400-msec depolarization at −30 mV. Fits (*dashed lines*) obtained using one (*top*), two (*middle*) or three (*bottom*) sequential open states are shown superimposed to the current traces. The values of the rate constants are shown inside the boxed kinetic schemes. Averaged data from six oocytes are indicated. Weighted sum of squared errors between fit and experimental data (*W.S.S.*) is shown on the graphs. The percentage of occupation of the different open states amounted to 75% for *O4* and 25% for *O5*. (*D*) Fits to tail current following depolarization to +40 mV. Note the reduction of residuals for the three-open-states fit as compared with the fit with only two open states when currents are obtained following depolarizations at +40 mV, but not at −30 mV. Further reductions in *W.S.S.* were not observed at +40 mV by increasing the order of the model with an additional *O7* open state. Occupation percentages correspond to 69% for *O4*, 21% for *O5* and 10% for *O6*. Similar results were obtained in the five additional oocytes analyzed.

et al., 2000) not only slows down deactivation, but tends to drive HERG channels to additional and more distal open states. It also suggests that these additional states correspond to channel conformations from which slow deactivation takes place upon repolarization.

It is important to note that these differences do not represent an artifactual error of the clamping procedure due to the enhanced current magnitude as the depolarization levels are increased since: a) analysis of current decay was limited to cells showing tail currents at negative voltages (−100 mV) that did not surpass 5–6 μA; b) similar changes in kinetics were not detected in oocytes expressing mutant channels such as Δ138–373 that showed similar current levels (*see below*); c) maintenance of the initial electrode resistance was periodically checked during the recordings without moving the electrodes from the cell, using the circuit provided by the amplifier, and d) data analysis was restricted to wild-type and mutant channels expressed in oocytes of the same batch in which the same electrodes were used to measure the currents.

The behavior of proximal domain-deleted channels when compared with a similar procedure is shown in Fig. 6. Unlike with full-length channels, a three-open-states model was necessary to adequately fit the tail-current time course, even after depolarization steps to quite negative voltages, at which little activation is attained. This indicates that channels without the proximal domain move more easily through the activation pathway up to the more distal open states. It also suggests that the presence of this domain not only slows down transitions between closed states, but also tends to delay the arrival of the channels to state(s) showing slower rates of deactivation.

Specific Alteration of the HERG Initial Segment in the Amino Terminus Modifies Channel Closing but Does not Affect Activation Kinetics

Previous work from our laboratory suggested that the presence of the proximal domain constrained the effective interaction of the *eag*/PAS domain with the channel core, and that this interaction was dependent on channel opening (Viloria et al., 2000). It is also known that the slow deactivation characteristic of HERG depends on the presence of an *eag*/PAS domain interacting with the channel core (Wang et al., 1998, 2000; Cabral et al., 1998; Sanguinetti & Xu, 1999). This prompted us to check whether entrance in the more distal open states could be related to such an interaction of the *eag*/PAS domain with the channel. For this purpose, we generated a variant of the channel containing an intact proximal domain that could maintain unaltered its activation properties, but carrying a modification of the *eag*/PAS domain that could preclude the progression up to the more distant open states.

Unlike other variants carrying small deletions in the initial sequence of the *eag*/PAS domain, good expression levels equivalent to those of wild-type channels were obtained with a construct containing a short stretch of amino acids (corresponding to an HA epitope, *see* Methods) at the beginning of the amino terminus. As shown in Fig. 7, introduction of the HA epitope does not modify the HERG voltage dependence of activation. Furthermore, both the initial delay in the current records and the rate constant for the slowest voltage-independent transition along the activation sequence remained almost unaffected by introduction of such an additional sequence. However, this lack of effect on activation contrasts with the clear accelerations of deactivation observed in the presence of the epitope (Fig. 8). Thus, prominent differences in both the fast and the slow components of current decay were observed up to −100 mV. The acceleration of closing extended to more negative potentials when only the fastest component of deactivation (a component that otherwise accounted for near ninety per cent of the current at these voltages) was considered. Nevertheless, the voltage dependence of the deactivation rates was smaller in H3HA than in wild-type channels. This tended to equal the tail current kinetics at very negative voltages. Analogous results were obtained with H3HA channels inactivating normally without the S620T mutation (*not shown*). These results add further support to our previous conclusion that whereas the *eag*/PAS domain mainly controls current deactivation, the activation properties of HERG are largely set by the proximal domain (Viloria et al., 2000).

HERG Channels Modified in the *eag*/PAS Domain do not Reach the Farthest Open States that Determine Slower Deactivation Rates

As indicated above, the presence of multiple open states can be demonstrated by the slowing of the deactivation time course in response to activating pulses of increasing magnitude and/or duration. In the following, we studied the deactivation time course of the H3HA channels following activation pulses to different potentials, fitting the tail current records to models containing increasing numbers of open states. As shown in Fig. 9, a two-open-states model provided the best fit to tail currents, regardless of the previous voltage (−40 or +40 mV) used to activate the channels. This strongly contrasts with the results obtained with either wild-type or proximal domain-deleted channels, since in these cases closing always takes place from a third open state when depolarizing

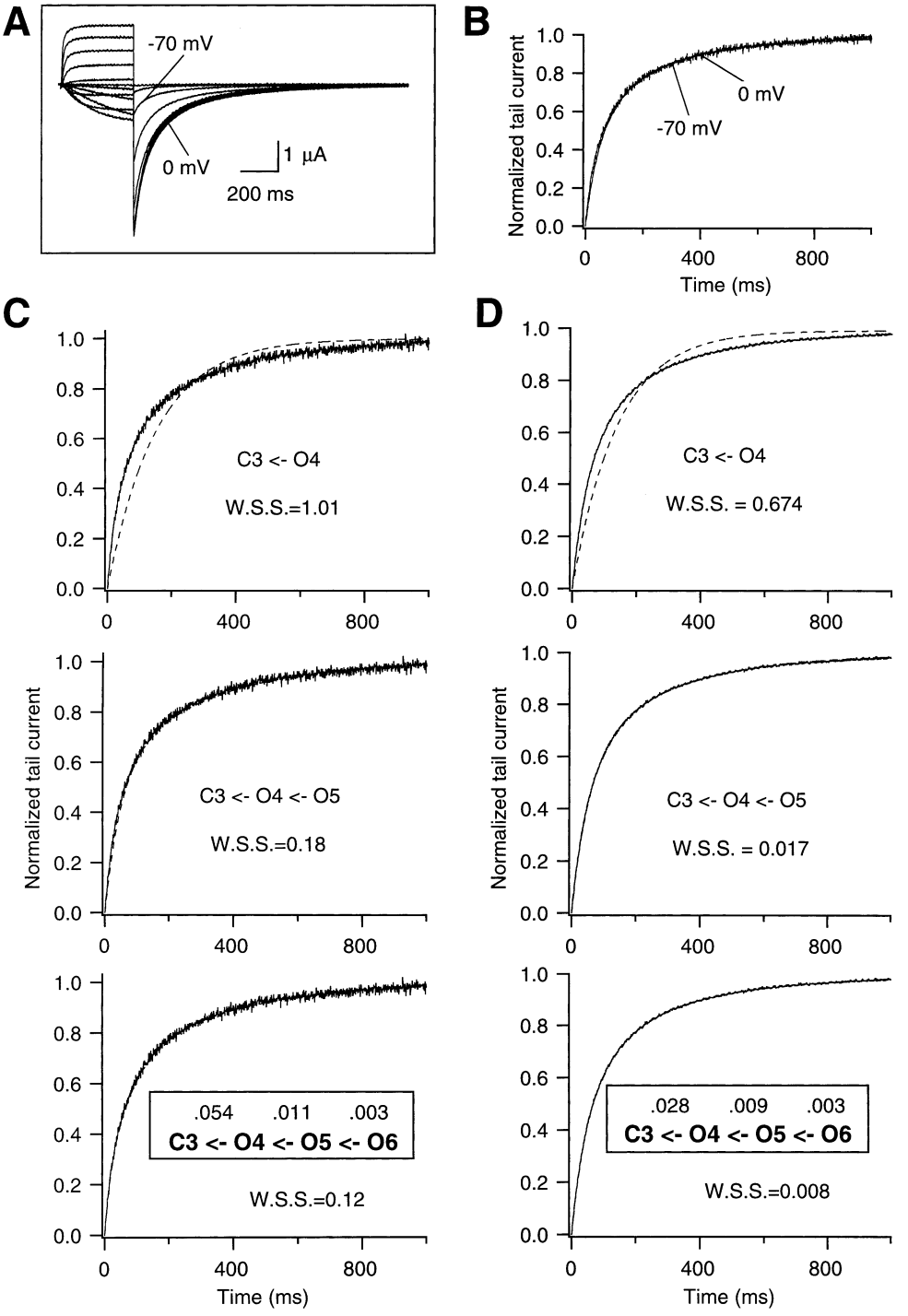

Fig. 6. Fitting of models with different number of open states to Δ138–373 HERG deactivating tail currents as a function of previous depolarization voltage. (*A*) Family of currents in response to 0.4-sec depolarizations between −90 and 0 mV followed by 1-sec repolarizations to −110 mV. High-K^+ extracellular medium with 50 mM KCl was used. (*B*) Comparison of time course of tail currents recorded in response to depolarizing pulses to −70 and 0 mV. Normalized tail currents are shown corresponding to traces plotted in panel *A*. (*C*) Fits to time course of the tail current recorded at −100 mV following the 400-msec depolarization at −70 mV. Fits (*dashed lines*) obtained using one (*top*), two (*middle*) or three (*bottom*) sequential open states are shown superimposed to the current traces. The averaged values of the rate constants from the five analyzed cells are shown inside the boxed kinetic schemes. Occupation percentages correspond to 36% for *O4*, 43% for *O5* and 20% for *O6*. (*D*) Fits to tail current following depolarization to zero mV. Note the relatively negative potentials used to activate the channels to compensate the shift in activation voltage dependence caused by the proximal domain deletion (Viloria et al., 2000). Occupation percentages corresponded to 53% for *O4*, 33% for *O5* and 14% for *O6*. Similar results were obtained in four additional oocytes.

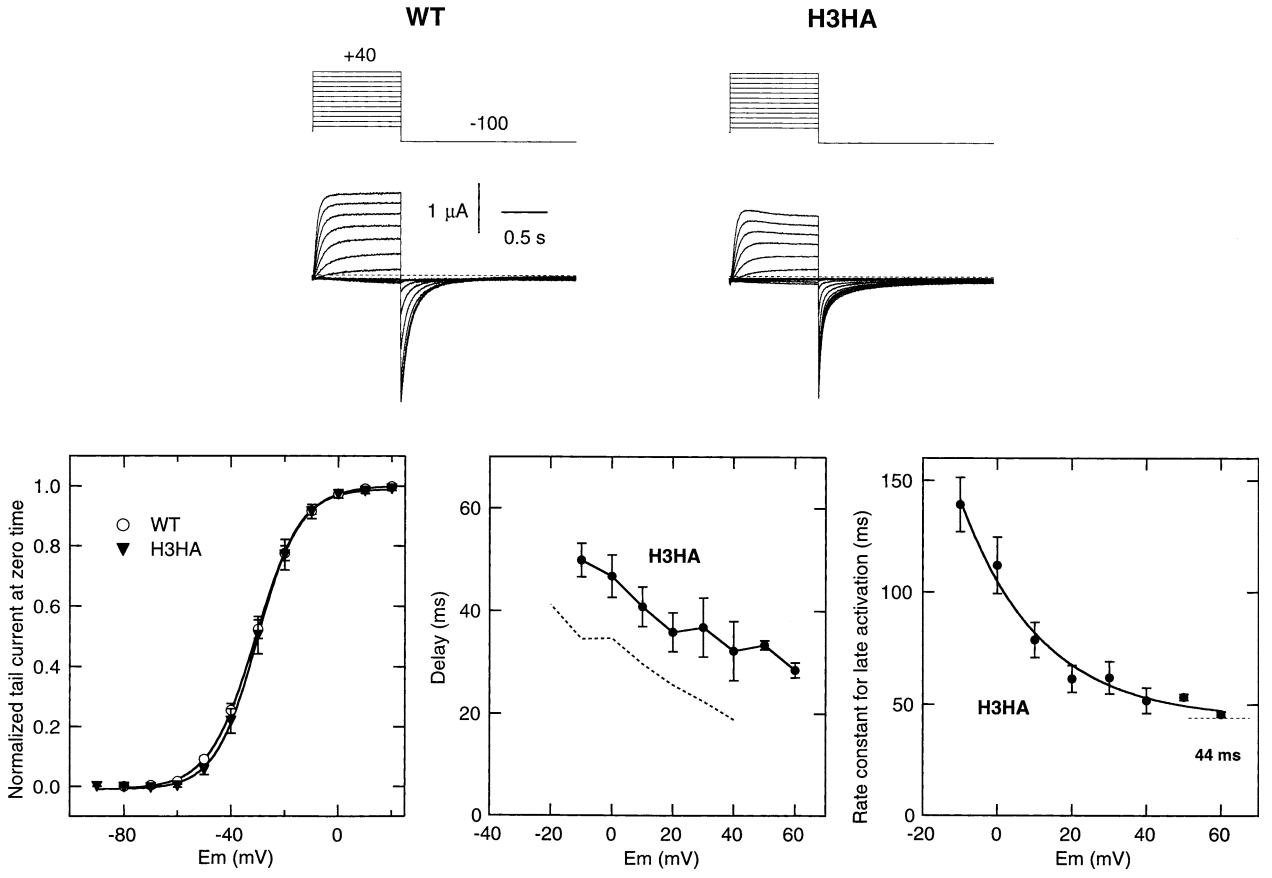

Fig. 7. Characterization of activation kinetics in H3HA channels. Families of currents with 1-sec steps to different voltages applied to non-inactivating channels carrying (H3HA) or not (WT) an HA epitope at the beginning of the amino terminus, are shown at the top. The voltage dependencies of activation under those conditions are shown in the lower left panel. The continuous lines correspond to Boltzmann curves, $h(V) = I_{max}\ [1/(1 + \exp((V - V_{half})/k))]$, that best fitted the data. Values from eight oocytes from three animals are used. The delay in activation and the time constants obtained from single-exponential fits to the late phase of activation following the procedures described in the legends of Figs. 1 and 2, are shown in the middle and right lower panels, respectively. Dotted lines representing the variation of activation rates for wild-type channels as in Figs. 1 and 2 are also shown for comparison. No significant differences ($p > 0.05$) between the data points for wild-type and H3HA channels were detected, except in the two values of delay corresponding to +10 and +20 mV (Student's *t*-test).

steps to positive (+40 mV) potentials are used (*see above*). The coincidence of fast deactivation and two predicted open states both in wild-type channels at low voltages and in H3HA at all potentials, and the prediction of three open states in Δ138–373 channels or strongly depolarized wild-type channels showing equal slowly deactivating kinetics (Viloria et al., 2000), further emphasizes the validity of kinetic modeling to detect the presence of additional open states, even in cases such as the proximal domain-deleted constructs, in which deactivation slowing can not be used as an additional argument for this purpose. Furthermore, our data indicates that HERG channels carrying a modified *eag*/PAS domain are unable to reach the third open state from which deactivation proceeds slowly, even at the positive voltages and depolarization times at which the constraints imposed by the presence of the proximal domain are overcome.

Discussion

Inwardly rectifying properties of HERG-like channels are an essential determinant of their physiological role in a variety of cells. Important contributors to this properties are: a) a slow deactivation rate upon repolarization, leading to prominent tail currents produced by reopening of the channels as they rapidly recover from inactivation, before slowly closing, and b) a reduced depolarization-induced current due to superposition of slow activation and fast inactivation (Trudeau et al., 1995; Sanguinetti et al., 1995; Schönherr & Heinemann, 1996; Smith et al., 1996; Spector et al., 1996b; Wang et al., 1997). Besides a rapid inactivation, a slow activation rate constitutes a crucial factor limiting the outward flow of K^+ ions, thus contributing to maintenance of the plateau potential in cardiac cells (Hancox, Levi & Witchel, 1998). Without it a rapidly activating (and inactivat-

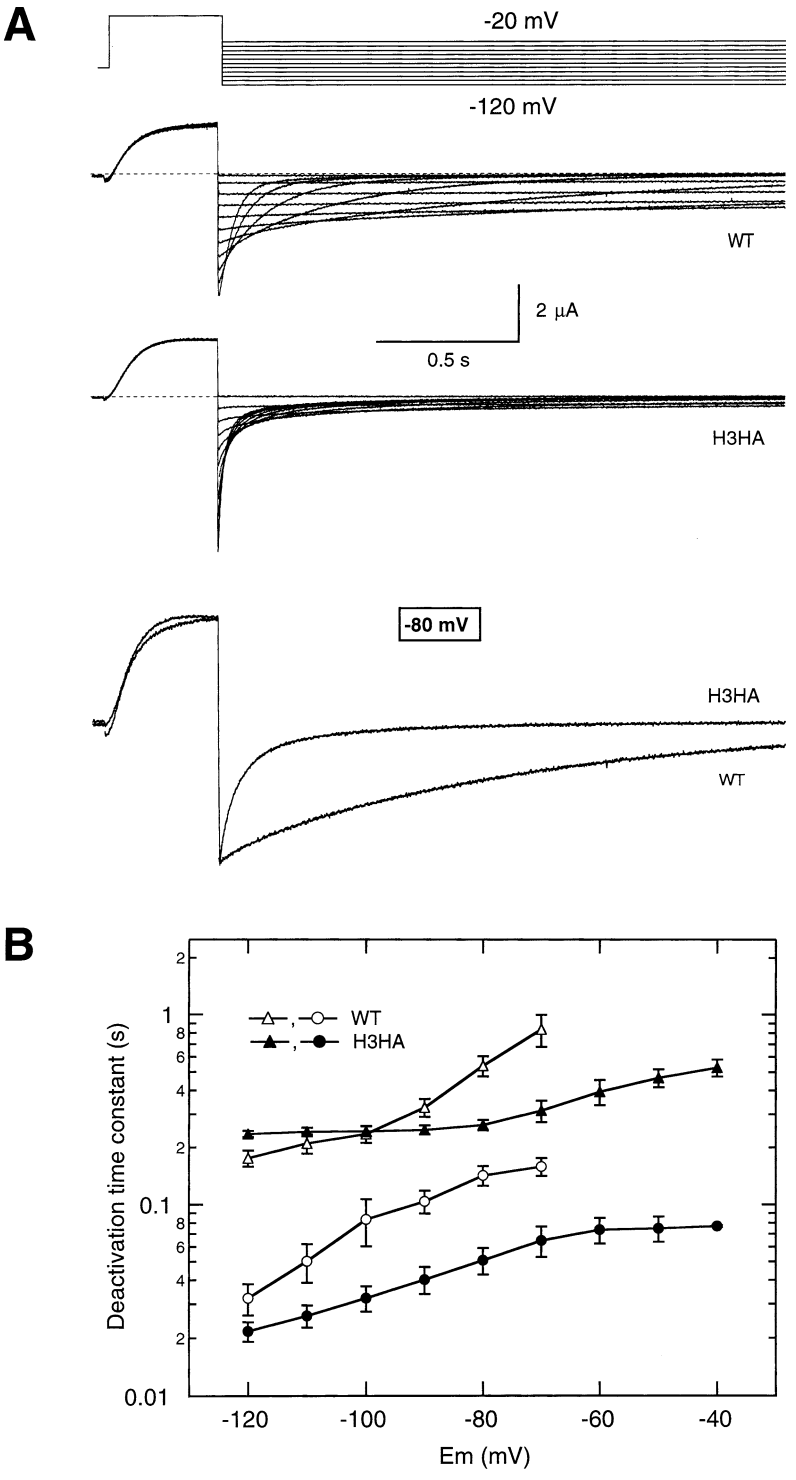

Fig. 8. Effect of the HA epitope at the beginning of the amino terminus on HERG channel deactivation rates. (*A*) Families of currents from channels with (H3HA) and without (WT) the HA epitope in the amino terminus. Currents were obtained during steps to potentials ranging from −120 to −20 mV, following depolarizing pulses to +40 mV, as indicated at the top of the traces. High-K^+ extracellular medium with 50 mM KCl was used to maximize tail current magnitudes. The zero-current level is indicated by the dashed lines. Scaled tail currents obtained at −80 mV are also shown superimposed to visualize better the differences in the decay time course. (*B*) Fast (*circles*) and slow (*triangles*) deactivation time constants as a function of repolarization voltage. Deactivation time constants were quantified by fitting a double exponential to the decaying portion of the tails. Data from three to nine oocytes from three frogs are averaged on the graphs.

ing) A-type current would be obtained. Slow activation also seems to participate in use-dependent current accumulations implicated in spike-frequency accommodation of neuronal firing (Schönherr et al., 1999). Nevertheless, the molecular determinant(s) of HERG activation slowness are still poorly defined. In a recent paper we recognized an important contribution of a HERG-specific proximal domain located in the amino terminus to slow activation gating (Viloria et al., 2000). However, apart from a clear influence of proximal domain removal on the time constant of the slowest voltage-independent transition between closed states, the effect of the deletion on other specific kinetic transitions remained obscure. In an attempt to further correlate the presence of specific amino-terminal structures with distinctive molecular transi-

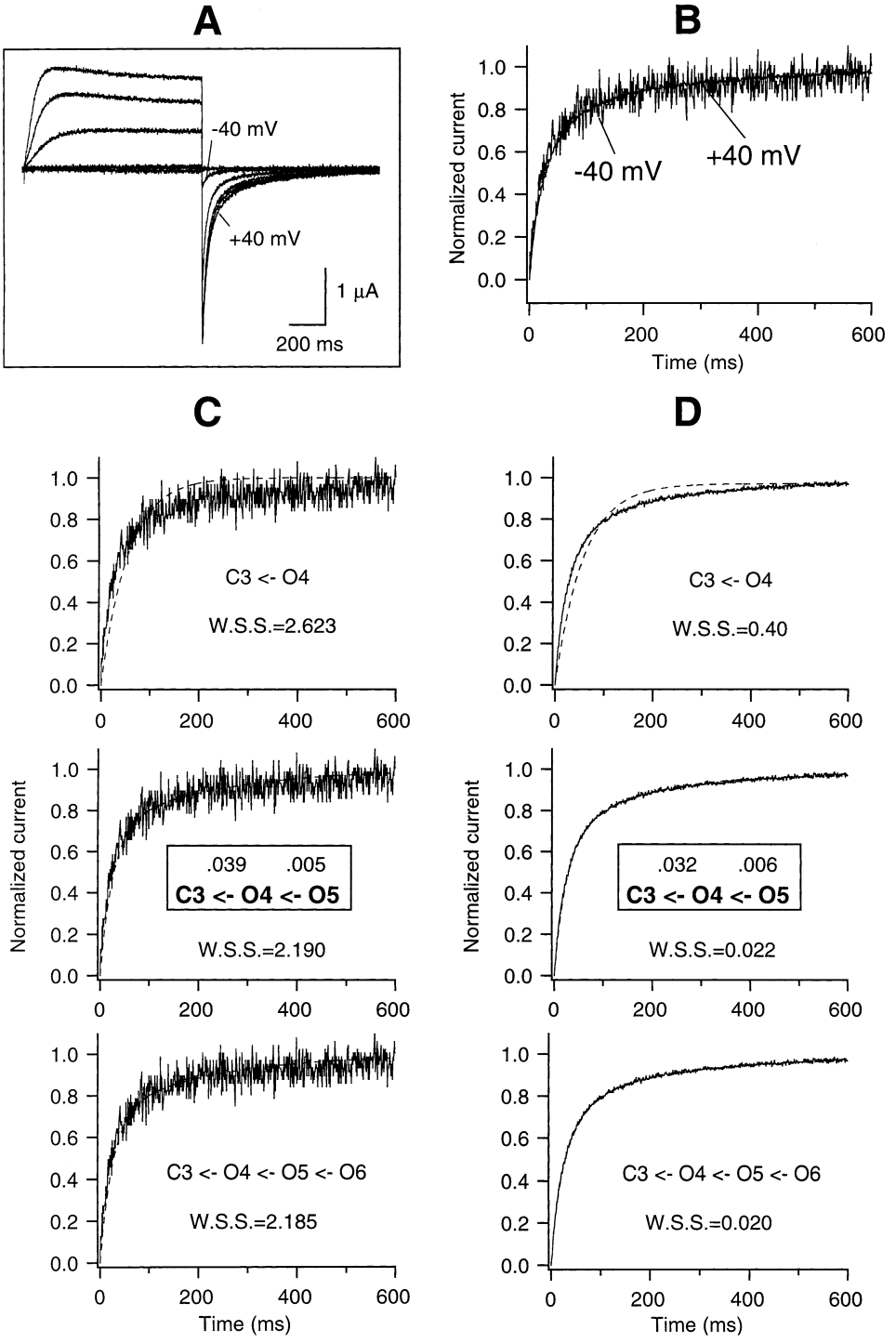

Fig. 9. Fitting of models with different number of open states to H3HA HERG deactivating tail currents as a function of previous depolarization voltage. (*A*) Family of currents in response to 1-sec depolarizations between −60 and +40 mV in 20 mV increments followed by 1-sec repolarizations to −100 mV. High-K^+ extracellular medium with 50 mM KCl was used to maximize tail current magnitude at negative repolarizing voltages. (*B*) Comparison of time course of tail currents recorded in response to depolarizing pulses to −40 and +40 mV. Normalized tail currents are shown corresponding to traces plotted in panel *A*. (*C*) Fits to time course of the tail current recorded at −100 mV following the 400-msec depolarization at −40 mV. Fits (*dashed lines*) obtained using one (*top*), two (*middle*) or three (*bottom*) sequential open states are shown superimposed to the current traces. Occupation percentages corresponded to 73% for *O4*, and 27% for *O5*. (*D*) Fits to tail current after depolarization at +40 mV. Occupation percentages correspond to 70% for *O4*, and 29% for *O5*. Similar results were obtained in five additional oocytes.

tions, we checked here the effect of proximal and *eag*/PAS domain alterations in individual transitions along the HERG activation pathway.

Opening of HERG channels constitutes a multistep sequential process in which the final and voltage-dependent closed-to-open transition is preceded by two steps between closed states, the initial one being weakly voltage-dependent and the second one essentially voltage-independent (Wang et al., 1997, 1998; Kiehn et al., 1999). The introduction of a threonine in position 620 (HERG S620T) completely removes inactivation (Ficker et al., 1998) without any modification of activation properties (Viloria et al., 2000), making it easy to perform measurements of gating parameters without contamination with inactivation processes. Using this S620T variant, we detected a clear acceleration of activation rates upon removal of the proximal domain. The acceleration was manifested in all forward transitions, including both voltage-dependent and -independent steps. This could be expected if the proximal domain does not constitute a component of the voltage-dependent gating machinery, but acts either as a brake for transmission of the voltage sensor molecular movement to the gate structure(s) or as a constraining factor for operation of the gate itself. The intracellular loop between the S4 and S5 transmembrane segments of HERG has been regarded as an important domain linking the movement of the S4 to channel opening and acting as a docking site for regulation of channel deactivation by the *eag*/PAS domain (Wang et al., 1998, 2000; Sanguinetti & Xu, 1999). The possibility that the proximal domain constrains the molecular conduction of the opening signal is suggested by our recent data indicating that several mutational alterations in the end of the S4 or in the S4-S5 linker are able to revert the accelerating effects of proximal domain removal (C.G. Viloria, P. de la Peña and F. Barros, *unpublished*). Unfortunately, most of these mutations also cause important alterations in the level of expression and/or the activation properties (*see also* Sanguinetti & Xu, 1999), imposing strong limitations in the interpretation of the data. Clearly, further work would be necessary to correlate any structural rearrangement in the amino terminus with the different individual transitions between closed states.

In addition to several closed states, our data support a kinetic model for the non-inactivating full-length HERG in which the latest closed state is followed by three kinetically distinguishable open states. A key factor in favor of such an interpretation is that a progressive slowing of tail current decay is induced when the duration and/or the magnitude of previous depolarization pulses is increased (Viloria et al., 2000). Although a multi-exponential tail current decay can be modeled with either multiple closed states or with multiple open states (Correa & Bezanilla, 1994, Zagotta et al., 1994), a multiple-open-states system would be required to explain the dependence of the deactivation time course on the strength of the activating pulses (Rich & Snyders, 1998). The use of a channel variant from which inactivation has been totally removed (Ficker et al., 1998) also excludes the possibility that such a slowing is caused by recovery from either a rapid (hidden) inactivation state or a voltage-independent form of flicker-inactivating state (Rich & Snyders, 1998).

A molecular correspondence to the different open states can be inferred from the analysis of deactivation using channel variants in which the functionality of the proximal domain or the *eag*/PAS domain has been selectively impaired. Elimination of the proximal domain does not modify any of the deactivation parameters as compared to wild-type channels, providing that these are allowed to complete their activation sequence at long times or strong depolarizations. Interestingly, the only detectable difference between these two channel types is manifested at depolarization levels at which full activation has not been reached. Thus, whereas a two-open-states model can adequately describe the behavior of wild-type channels at negative voltages at which little activation is achieved, a three-open-states model equivalent to that describing deactivation of fully activated channels is necessary to account for the deactivation kinetics of proximal domain-deleted channels only marginally activated at scarcely depolarize potentials. Among the previously demonstrated slowing of channel closing following interaction of the *eag*/PAS domain with the channel core (Cabral et al., 1998; Wang et al., 1998; Sanguinetti & Xu, 1999) this indicates that the farther and slower deactivating open states correspond to those in which the *eag*/PAS domain-channel interaction takes place. It also adds further support to our conclusion that reorganization of the proximal domain is important not only for progress of channel opening, but also for productive interaction of the *eag*/PAS domain with the channel and subsequent slowing of deactivation (Viloria et al., 2000). A final demonstration that this is indeed the case is provided by our data using H3HA channels in which the *eag*/PAS domain has been functionally blocked. In this case, essentially equal activation properties as those of wild-type channels are observed. However, only fast deactivation rates and kinetic characteristics proper of a two-open-states model are obtained regardless of the strength of the activating pulses.

In summary, our results indicate that the HERG channel has multiple closed and open states and that the presence of the HERG-specific proximal domain slows both activation gating and entry in the later open states that limit the rate of deactivation. Note, however, that the more distal open states reported here may correspond to non-conductive states in the

natural HERG, rapidly inactivating without the S620T mutation (Olcese et al., 2001). The correspondence of the individual open states described here with the two different open states previously reported from open-time distributions of single-channel data (Zou et al., 1997) is also unclear. Finally, among previous results (Viloria et al., 2000), our data also indicate that two different domains exist in the amino terminus regulating HERG gating; an *eag*/PAS domain mainly controlling current deactivation and a proximal domain regulating current activation, but indirectly also deactivation due to its ability to constrain the influence of the interaction of the *eag*/PAS domain with the gating machinery. Note also that although the term *eag*/PAS has been used in this work to refer to the whole stretch of amino acids that extends from residues 1 to 138, two functionally distinguishable subdomains may exist on it: a subdomain structurally identical to a eukaryotic PAS domain (Cabral et al., 1998) and an initial segment of 16–25 residues with undetermined structure that could constitute a crucial point of control of deactivation (Wang et al., 2000), but not of inactivation kinetics (Wang et al., 1998). It would be interesting to know if these functionally discrete protein domains play a role in specific regulation of channel properties by physiologically relevant auxiliary subunits (Abbott et al., 1999) or hormonal stimuli (Barros et al., 1998; Kiehn, 2000).

We thank Dr. E. Wanke for providing the HERG channel-containing plasmid and Dr. E. Fernández for help with statistical analysis. D. G-V was supported by the Fundación Inocente, Madrid, Spain. T.G. holds a predoctoral fellowship from F.I.S. of Spain (Ref. No. 99/9298). J.G. is a predoctoral fellow from FICYT of Asturias (Ref. No. BP00-057). This work was supported by grants PB96-0316 and PM99-0152 from DGICYT of Spain.

References

Abbott, G.W., Sesti, F., Splawski, I., Buck, M.E., Lehmann, M.H., Timothy, K.W., Keating, M.T., Goldstein, S.A.N. 1999. MiRP1 forms I_{Kr} potassium channels with HERG and is associated with cardiac arrhythmia. *Cell* **97:**175–187

Akbarali, H.I., Thatte, H., He, X.D., Giles, W.R., Goyal, R.K. 1999. Role of HERG-like K^+currents in opossum esophageal circular smooth muscle. *Am. J. Physiol.* **277:**C1284–C1290

Barros, F., Villalobos, C., García-Sancho, J., del Camino D., de la Peña P. 1994. The role of the inwardly rectifying K^+ current in resting potential and thyrotropin-releasing hormone-induced changes in cell excitability of GH3 rat anterior pituitary cells. *Pfluegers Arch.* **426:**221–230

Barros, F., del Camino D., Pardo, LA., Palomero, T., Giráldez, T., de la Peña, P. 1997. Demonstration of an inwardly rectifying K^+ current component modulated by thyrotropin-releasing hormone and caffeine in GH3 rat anterior pituitary cells. *Pfluegers Arch.* **435:**119–129

Barros, F., Gómez-Varela, D., Viloria, C.G., Palomero, T., Giráldez, T., de la Peña, P. 1998. Modulation of human erg K^+ channel gating by activation of a G protein-coupled receptor and protein kinase C. *J. Physiol.* **511:**333–346

Bauer, C.K., Schäfer, R., Schiemann, D., Reid, G., Hanganu, I., Schwarz J.R. 1999. A functional role of the erg-like inward-rectifying K^+ current in prolactin secretion from rat lactotrophs. *Mol. Cell. Endocrinol.* **148:**37–45

Cabral, J.H.M., Lee, A., Cohen, S.L., Chait, B.T., Li, M, MacKinnon, R. 1998. Crystal structure and functional analysis of the HERG potassium channel N terminus: a eukariotic PAS domain. *Cell* **95:**649–655

Cherubini, A., Taddei, G.L., Crociani, O., Paglierani, M., Buccoliero, A.M., Fontana, L., Noci, I., Borri, P., Borrani, E., Giachi, M., Becchetti, A., Rosati, B., Wanke, E., Olivotto, M., Arcangeli, A. 2000. HERG potassium channels are more frequently expressed in human endometrial cancer as compared to non-cancerous endometrium. *Br. J. Cancer* **83:**1722–1729

Colquhoun, D., Hawkes, A.G. 1995. A Q-matrix cookbook: how to write only one program to calculate the single-channel and macroscopic predictions for any kinetic mechanism. *In:* Single channel recording. 2nd ed. B. Sakmann, E. Neher, editors, pp. 589–633. Plenum, New York.

Correa, A.M., Bezanilla, F. 1994. Gating of the squid sodium channel at positive potentials. I. Macroscopic ionic and gating currents. *Biophys. J.* **66:**1853–1863

Curran, M.E., Splawski, I., Timothy, K.W., Vincent, G.M., Green, E.D., Keating, M.T. 1995. A molecular basis for cardiac arrhythmia: HERG mutations cause long QT syndrome. *Cell* **80:**795–804

Cushman, S.J., Nanao, M.H., Jahng, A.W., DeRubies, D., Choe, S., Pfaffinger, P.J. 2000. Voltage dependent activation of potassium channels is coupled to T1 domain structure, *Nat. Struct. Biol.* **7:**69–77

De la Peña, P., Delgado, L.M., del Camino, D., Barros, F. 1992. Cloning and expression of the thyrotropin-releasing hormone receptor from GH_3 rat anterior pituitary cells. *Biochem. J.* **284:**891–899

Emmi, A., Wenzel, H.J., Schwartzkroin, P.A, Taglialatela, M., Castaldo, P., Bianchi, L., Nerbonne, J., Robertson, G.A., Janigro, D. 2000. Do glia have heart? Expression and functional role for *Ether-a-go-go* currents in hippocampal astrocytes. *J. Neurosci.* **20:**3915–3925

Ficker, E., Jarolimek, W., Kiehn, J., Baumann, A., Brown, A.M. 1998. Molecular determinants of dofetilide block of HERG K^+ channels. *Circ. Res.* **82:**386–395

Gonzalez, C., Rosenman, E., Bezanilla, F., Alvarez, O., Latorre, R. 2000. Modulation of the *Shaker* K^+ channel gating kinetics by the S3-S4 linker. *J. Gen. Physiol.* **115:**193–207

Hancox, J.C., Levi, A.J., Witchel, H.J. 1998. Time course and voltage dependence of expressed HERG current compared with native "rapid" delayed rectifier K current during the cardiac ventricular action potential. *Pfluegers Arch.* **436:**843–853

Hoshi, T., Zagotta, W.N., Aldrich, R.W. 1990. Biophysical and molecular mechanisms of Shaker potassium channel inactivation. *Science* **250:**533–538

Irvine, L.A., Jafri, M.S., Winslow, R.L. 1999. Cardiac sodium channel Markov model with temperature dependence and recovery from inactivation. *Biophys. J.* **76:**1868–1885

Kiehn, J. 2000. Regulation of the cardiac repolarizing HERG potassium channel by protein kinase A. *Trends Cardiovasc. Med.* **10:**205–209

Kiehn, J.A., Lacerda, E., Brown, A.M. 1999. Pathways of HERG inactivation. *Am. J. Physiol.* **277:**H199–H210

Liu, S., Rasmusson, R.L., Campbell, D.L., Wang, S., Strauss, H.C. 1996. Activation and inactivation kinetics of an E-4031-sensi-

tive current from single ferret atrial myocytes. *Biophys. J.* **70:**2704–2715

Marten, I., Hoshi, T. 1997. Voltage-dependent gating characteristics of the K^+channel KAT1 depend on the N and C termini. *Proc. Natl. Acad. Sci. USA* **94:**3448–3453

Minor, Jr., D.L., Lin, Y.-F., Mobley, B.C., Avelar, A., Jan, Y.N., Jan, L.Y., Berger, J.M. 2000. The polar T1 interface is linked to conformational changes that open the voltage-gated potassium channel. *Cell* **102:**657–670

Olcese, R., Sigg, D., Latorre, R., Bezanilla, F., Stefani, E. 2001. A conducting state with properties of a slow inactivated state in a *Shaker* K^+ channel mutant. *J. Gen. Physiol.* **117:**149–163

Overholt, J.L., Ficker, E., Yang, T., Shams, H., Bright, G.R., Prabhakar, N.R. 2000. HERG-like potassium current regulates the resting membrane potential in glomus cells of the rabbit carotid body. *J. Neurophysiol.* **83:**1150–1157

Pascual, J.M., Shieh, C.-C., Kirsch, G.E., Brown, A.M. 1997. Contribution of the NH_2 terminus of Kv2.1 to channel activation. *Amer. J. Physiol.* **273:**C1849–C1858

Rich, T.C., Snyders, D.J. 1998. Evidence for multiple open and inactivated states of the hKv1.5 delayed rectifier. *Biophys. J.* **75:**183–195

Roden, D.M., Lazzara, R., Rosen, M., Schwartz, P.J., Towbin, J., Vincent, G.M. 1996. Multiple mechanisms in the long-QT syndrome: Current knowledge, gaps, and future directions. *Circulation* **94:**1996–2012

Rosati, B., Marchetti, P., Crociani, O., Lecchi, M., Lupi, R., Arcangeli, A., Olivotto, M., Wanke, E. 2000. Glucose- and arginine-induced insulin secretion by human pancreatic β-cells: the role of HERG K^+ channels in firing and release. *FASEB J.* **14:**2601–2610

Sanguinetti, M.C., Jiang, C., Curran, M.E., Keating, M.T. 1995. A mechanistic link between an inherited and an acquired cardiac arrhythmia: HERG channel encodes the IK_r potassium channel. *Cell* **81:**299–307

Sanguinetti, M.C., Xu, Q.P. 1999. Mutations of the S4–S5 linker alter activation properties of HERG potassium channels expressed in *Xenopus* oocytes. *J. Physiol.* **514:**667–675

Schäfer, R., Wulfsen, I., Behrens, S., Weinsberg, F., Bauer, C.K., Schwarz, J.R. 1999. The erg-like current in rat lactotrophs. *J. Physiol.* **518:**401–416

Schönherr, R., Rosati, B., Hehl, S., Rao, V.G., Arcangeli, A, Oiivotto, M., Wanke, E. 1999. Functional role of the slow activation property of ERG K^+ channels. *Eur. J. Neurosci.* **11:**753–760

Schönherr, R., Heinemann, S.H. 1996. Molecular determinants for activation and inactivation of HERG, a human inward rectifier potassium channel. *J. Physiol.* **493:**635–642

Schoppa, N.E., Sigworth, F.J. 1998. Activation of *Shaker* potassium channels. Characterization of voltage-dependent transitions. *J. Gen. Physiol.* **111:**271–294

Smith, P.L., Baukrowitz, T., Yellen, G. 1996. The inward rectification mechanism of the HERG cardiac potassium channel. *Nature* **379:**833–836

Spector, P.S., Curran, M.E., Keating, M.T., Sanguinetti, M.C. 1996*a*. Class III antiarrhythmic drugs block HERG, a human cardiac delayed rectifier K^+ channel. *Circ. Res.* **78:**499–503

Spector, P.S., Curran, M.E., Zou, A., Keating, M.T., Sanguinetti, M.C. 1996*b*. Fast inactivation causes rectification of the I_{Kr} channel. *J. Gen. Physiol.* **107:**611–619

Terlau, H., Heinemann, S.H., Stühmer, W., Pongs, O., Ludwig, J. 1997. Amino terminal-dependent gating of the potassium channel rat eag is compensated by a mutation in the S4 segment. *J. Physiol.* **502:**537–543

Trudeau, M.C., Warmke, J.W., Ganetzky, B., Robertson, G.A. 1995. HERG, a human inward rectifier in the voltage-gated potassium channel family. *Science* **269:**92–95

Viloria, C.G., Barros, F., Giráldez, T., Gómez-Varela, D., de la Peña, P. 2000. Differential effects of amino-terminal distal and proximal domains in the regulation of human *erg* K^+ channel gating. *Biophys. J.* **79:**231–246

Wang, J., Myers, C.D., Robertson, G.A. 2000. Dynamic control of deactivation gating by a soluble amino-terminal domain in *HERG* K^+ channels. *Biophys. J.* **115:**749–758

Wang, J., Trudeau, M.C., Zappia, A.M., Robertson, G.A. 1998. Regulation of deactivation by an amino terminal domain in *Human ether-a-go-go-related gene* potassium channels. *J. Gen. Physiol.* **112:**637–647

Wang, S., Liu, S., Morales, M.J., Strauss, H.C., Rasmusson, R.L. 1997. A quantitative analysis of the activation and inactivation kinetics of HERG expressed in *Xenopus* oocytes. *J. Physiol.* **502:**45–60

Warmke, J.W., Ganetzky, B. 1994. A family of potassium channel genes related to *eag* in *Drosophila* and mammals. *Proc. Natl. Acad. Sci. USA* **91:**3438–3442

Zagotta, W.N., Hoshi, T., Dittman, J., Aldrich, R.W. 1994. *Shaker* potassium channel gating. II. Transitions in the activation pathway. *J. Gen. Physiol.* **103:**279–319

Zhou, Z., Gong, Q., Ye, B., Fan, Z., Makielski, J.C., Robertson, G.A., January, C.T. 1998. Properties of HERG channels stably expressed in HEK 293 cells studied at physiological temperature. *Biophys. J.* **74:**230–241

Zou, A., Curran, M.E., Keating, M.T., Sanguinetti, M.C. 1997. Single HERG delayed rectifier K^+ channels expressed in *Xenopus* oocytes. *Am. J. Physiol.* **272:**H1309–H1314